jove

Establishing a Mouse Contusion Spinal Cord Injury Model Based on a Minimally Invasive Technique

Elham Yilizati-Yilihamu Elzat[1], **Xiangchuang Fan**[1], **Zimeng Yang**[1], **Zhongze Yuan**[1], **Yilin Pang**[2], **Shiqing Feng**[1,2]

[1] Department of Orthopaedics, Qilu Hospital of Shandong University [2] Department of Orthopaedics, Tianjin Medical University General Hospital

Corresponding Author

Shiqing Feng

shiqingfeng@sdu.edu.cn

Citation

Elzat, E.Y.Y., Fan, X., Yang, Z., Yuan, Z., Pang, Y., Feng, S. Establishing a Mouse Contusion Spinal Cord Injury Model Based on a Minimally Invasive Technique. *J. Vis. Exp.* (187), e64538, doi:10.3791/64538 (2022).

Date Published

September 7, 2022

DOI

10.3791/64538

URL

jove.com/video/64538

Abstract

Using minimally invasive methods to model spinal cord injury (SCI) can minimize behavioral and histological differences between experimental animals, thereby improving the reproducibility of the experiments.

These methods need two requirements to be fulfilled: clarity of the surgical anatomical pathway and simplicity and convenience of the laboratory device. Crucially for the operator, a clear anatomical pathway provides minimally invasive exposure, which avoids additional damage to the experimental animal during the surgical procedures and allows the animal to maintain a consistent and stable anatomical morphology during the experiment.

In this study, the use of a novel integrated platform called the SCI coaxial platform for spinal cord injury in small animals to expose the T9 level spinal cord in a minimally invasive way and stabilize and immobilize the vertebra of mice using a vertebral stabilizer is researched, and, finally, a coaxial gravity impactor is used to contuse the spinal cord of mice to approach different degrees of T9 spinal cord injury. Finally, histological results are provided as a reference for the readers.

Introduction

Traumatic spinal cord injury (SCI) easily predisposes the individual to severe consequences[1]; nevertheless, there is no effective treatment at present[1,2]. Animal contusion models are one of the major methods to study SCI[3,4].

From 2004 to 2014[4], rats were used as model organisms in 289 of 407 studies (71%) and mice in 69 (16.9%). Indeed, the proportion of experiments with mice has gradually increased over the years due to their advantages over other models, especially the great potential for gene regulation studies[3,4,5]. Therefore, more compatible tools are required to conduct more studies using the mouse as a model because of the great importance attached to model consistency[6]. The common devices reported in previous studies are basically based on Allen's spinal cord impact principle, for instance, the basic weight drop impactor[7,8], the New York University (NYU)/ Multicenter Animal Spinal Cord Injury

Studies (MASCIS) impactor[1,9], and the Infinite Horizon (IH) impactor[10,11]. The weight drop impactor and the NYU/MASCIS impactor share the same principle of aiming at the targeted spinal cord and dropping a fixed weight from different heights to make different injury severities. The IH impactor creates the spinal cord injury according to different forces.

For convenience in using the mouse model in SCI studies and to establish the basis for effective treatment methods, an integrated mouse spinal cord impact injury platform, called the spinal cord injury coaxial platform (SCICP), is developed. The platform consists of four main components: (1) an animal operating table designed for a suitable position for operated mice, which is very compact and provides convenience without position restriction; (2) a micro-retractor on both sides to hold the paravertebral muscles during operation; (3) a vertebral stabilizator to hold the vertebra before the procedure of SCI (two vertebral stabilizators are available for operation on larger animals such as rats); (4) a sleeve, an impactor tip, weights, and a pull pin. The three parts should be assembled to a removable X-Y-Z arm. For precise targeting, an impactor tip is placed on the surface of the spinal cord, and the X-Y-Z arm is gently descended to the expected height with the assistance of the mark between the impactor tip and the sleeve. The impactor tip is made of a 0.12 g aluminum alloy to avoid damage to the spinal cord ascribed to large weight compression before the procedure. The pull pin is for holding the weights on the top of the sleeve to prepare the weight drop (**Figure 1**).

In previous studies, impact force division was defined according to the IH device's impact force data, which are 30 Kdyn, 50 Kdyn, and 70 Kdyn, respectively[6,10]. During the research process, serial degrees of SCI models were proven to be established based on SCICP, which can be used in various studies. Therefore, before officially starting the experiment, the impact forces generated by various weights of different masses were tested using a peak pressure testing device. As a result, three standardized representative SCI mouse models were selected as three different degrees of injury, including graded mild, moderate, and severe groups, respectively[6,10], and the weights were released at the same height, with a 1.3 g weight for mild, 2.0 g for moderate, and 2.7 g for severe damage.

As another means to guarantee operability and accuracy, a novel and minimally invasive operative approach is reported. Through researching the anatomy of normal mice, a new method to locate the interspinous space of T12-T13 is found. The method of vertebra locating in the operation steps is easy to master and accurate, which ensures precise locating for minimally invasive operations.

Hopefully, this technique of contusion injury may aid the research and understanding of spinal cord injury, including pathophysiology comprehension, management evaluation, and so on.

Protocol

NOTE: All the experiments were approved by the Laboratory Animal Ethical and Welfare Committee of Shandong University Cheeloo College of Medicine (approval number: 21L60) and were performed according to the Guide for the Care and Use of Laboratory Animals published by the National Institutes of Health (NIH Publications No. 85-23, revised 1996).

1. Mechanism of the spinal cord injury coaxial platform and mechanical tests

1. Assemble the platform with a surgical operating table, a vertebral stabilizator, and an impactor tip (**Figure 1**).
   NOTE: Keep the weight drop and exhaust slots, which prevent the weight from encountering air currents, clean, because any dirt on the weight drop or sleeve could affect the precision of the platform.
2. Put the tip, which allows for accurate spinal cord locating, into the sleeve.
3. Select proper masses of the weight drops for the experiment, which are 1.3 g, 2.0 g, and 2.7 g for the mild, moderate, and severe groups, respectively.
4. Plug the pull pin into the holes of the weight drop.
5. Assemble the weight drop to the top of the sleeve with the pull pin fitted in the groove on the X-Y-Z arm so that, once the locating is complete, the weight is released to strike the impactor tip, consequently contusing the spinal cord, and changes in the spinal cord are observed under the microscope.
6. Adjust the removable 0.1 mm precision X-Y-Z arm for the operator's convenience to provide adequate working space (**Figure 1D, E**).
   NOTE: To confirm the consistency of the results of the study, before the experiment begins, measure the force generated when the weight is dropped inside the sleeve using a peak pressure detection device. A repeat of confirmation is not necessary for future studies.
7. Turn on the device, place the metal pressure receptor below the tip, zero the adapter, release the pull pin, and record the actual impact force.

2. Locating and laminectomy of the 9th thoracic vertebra (T9)

NOTE: Female C57BL/6J mice 9-10 weeks old were purchased from Jinan Pengyue Experimental Animal Company (Jinan, China).

1. Autoclave a suite of surgical instruments for the experiment and sterilize the operating table with 75% alcohol before surgery.
2. Inject buprenorphine for analgesia (0.05-2.0 mg/kg, SQ) 30 minutes before anesthesia for injury operations. Then, anesthetize the mouse with isoflurane (induction: ~3%-5%, maintenance: ~1.5%-2%). Check if the animal is fully anesthetized by the reflexes of tail or toe pinch. Once anesthesia is in effect, lay the mouse in a prone position in a designated part of the operating table and coat the cornea with ophthalmic ointment (apply ophthalmic ointment to the corneas to protect the eyes from drying during surgery).
   1. Shave the hair from the caudal to the rostral with an electric shaver over the thoracolumbar spine. Sterilize the skin several times in a circular motion with iodophor for 30 s and followed by 75% alcohol. Apply a sterile surgical drape and make a longitudinal incision of approximately 1.5 cm on the skin from approximately T6 to T13 with a scalpel and blade.
      NOTE: Palpate along the costal margin to the midline, where the T12-T13 interspinous space is located. Make a 1.5 cm incision to the rostral, and the incision is approximately flush with T6-T13 vertebrae.

3. Explore the 13th rib on one side from the bony portion under the operating microscope. Explore the spinous process in the midline by lightly touching the area of the costovertebral angle and then toward the rostral to locate the interspinous space of the T12-T13. Explore the interspinous space of the T9-T10 from the space of the T12-T13 to the rostral side. (**Figure 2A, 3A**)

4. Dissect the paraspinal muscle along the spinous process of the T9 to the anterior and posterior facet joints of both sides with micro scissors (**Figure 3B**). Retract the paraspinal muscles with micro-retractors and clean the soft tissue on the lamina and in the interspinous space of the T8-T9 and T9-T10 with micro scissors.

5. Perform T9 laminectomy, clamp the spinous process of T9 with microsurgery forceps, slightly lift it up, insert the micro scissors parallelly along the right dorsolateral side of the lamina, avoiding damage to the spinal cord, and cut off the lamina with micro scissors. Repeat on the left side, and the spinal cord can be exposed (**Figure 2B, 3C**).

6. Before fixing the vertebra, loosen the universal arm, and slowly clamp the 9th to 10th facet joints on both sides of the vertebra with the micro mosquito forceps of the vertebral stabilizator. Tighten the screws on the micro mosquito forceps, and the vertebra is thus stabilized. Adjust the spinal cord to the horizontal plane, tighten the universal arm, and the vertebra is fixed (**Figure 3D**).

3. T9 contusion injury

1. Once the T9 level spinal cord is exposed and the vertebra is fixed, aim at the spinal cord by the tip inside the sleeve under the operating microscopic (**Figure 3E**).

2. Check if the surface of the tip is parallel to the spinal cord from the posterior and lateral aspects of the spinal cord, since it is easy to observe the relationship between the spinal cord and the tip under the microscope, and that the operating table can be turned easily.

3. Check if the surface of the tip is parallel to the bilateral borders of the spared lamina before the tip is in contact with the spinal cord after the laminectomy since it is a natural reference plane parallel to the spinal cord.

4. After locating the interspinous space of the T12-T13, lower the sleeve until the end of the impactor is consistent with the mark on the observation window and the specified height of 22 mm is reached. Pull out the pull pin to release the weight (1.3 g, 2.0 g, or 2.7 g according to the group, with each group including 3 mice and each group having one mouse for each time point).
   NOTE: The spinal cord should be parallel to the ground and perpendicular to the tip; move the operating table to ensure the microscopic visual field, since the table is very compact.

5. Remove the impactor when the contusion is done and observe the degree of SCI under the operating microscope. In the mild group, a light red color alteration can be seen, while in the moderate group, the injury site exhibits dark red in 3-4 s, and, possibly, eminence can be observed. In the severe group, the dark red manifestations may appear immediately, and obvious eminence in the dura is manifested, but the dura is still in a consistent shape (**Figure 3F**).

6. Suture the superficial fascia and skin with sutures (polypropylene nonabsorbable suture, size: 6-0).

7. After completing the suture, sterilize the surgical area, place the mouse on a temperature-controlled pad until full consciousness is restored, and then put the mouse in the mouse cages.

4. Animal care

1. Place the animal on the heating pad for recovery and observe the movement of both hind limbs.
   NOTE: Animals that have undergone surgery should not be returned to the company of other animals until fully recovered.
2. Put a high-water diet on the cage floor so that animals can easily reach the food. Alternatively, use a cage with a lower feeding table.
3. Empty the mice's bladders twice a day after the operation because it is difficult for the moderate and severe injury groups to recover bladder function. Inject buprenorphine for analgesia (0.05-2.0 mg/kg, SQ) 8-12 h/day for 3 days.

5. Transcardial perfusion, staining, and immunostaining

1. On the 1st, 28th, and 56th days after injury, sacrifice one mouse of each group, respectively, by perfusion.
   1. Perfuse the mice with 60 mL of phosphate-buffered saline (PBS) and 20 mL of 4% paraformaldehyde after excessive anesthesia (4%-6% isoflurane).
   2. Collect the spine with micro scissors, extending rostrally and caudally 1 cm, respectively, from the lesion center.
   3. Resect the excess muscles, reserve intact spine segments with partial ribs for instruments to hold in step 5.1.4 and soak it in 4% paraformaldehyde for 24 h.
   4. Clamp the ribs with hemostatic forceps for fixation and define the lesion center under the microscope according to the resected lamina and color alteration in the lesion center of the spinal cord.
   5. Resect all the laminae and articular processes with micro scissors from the caudal.
   6. Cut off the nerve roots with micro scissors and take out the spinal cord.
   7. Collect 0.5 cm of the spinal cord extending caudally and rostrally, respectively, from the lesion center with micro scissors.
   8. Put the spinal cord in 30% sucrose at 4 ˚C for 48 h.
2. Cut the tissues into 6 µm thick sections after freezing according to histological examination type.
3. Perform hematoxylin and eosin (H&E) staining.
   1. Rewarm the sections to room temperature and soak the 6 µm thick sections in 4% formaldehyde for approximately 15 min, followed by soaking in 1x PBS for 1 min four times to remove residual OCT.
   2. Stain the sections with hematoxylin for 90 s, and rinse with double-distilled water.
   3. Then, wash the sections with running water for 3 min.
   4. Stain with eosin for 4 min and soak in 95% alcohol for 30 s twice to rinse excess eosin.
   5. Finally, dehydrate with gradient alcohol (95% alcohol and 50% alcohol once, successively) for 30 s and soak in xylene for transparency for 2 min. Then, seal the specimens with resin gel (coronal plane section: **Figure 4**; sagittal plane section: **Figure 5**).
4. Perform immunofluorescent staining.
   1. Rewarm the sections to room temperature and soak the 6 µm thick sections in 4% formaldehyde for approximately 2 min.
   2. Wash the sections in TBST for 5 min for three times.

3. Incubate the sections with blocking solution (10% goat normal serum in PBS) and block for 1 h to block non-specific binding of immunoglobulin.
4. Incubate the spinal cord sections overnight at 4 ˚C with both mouse anti-glia fibrillary acidic protein (GFAP, a marker for reactive astrocytes), polyclonal antibody (1:600), and rabbit anti-NF200 antibody (1:2000), a marker for neurofilament in 0.4 mL of blocking solution.
5. Rinse the sections with PBS and add 0.4 mL of blocking solution with Goat anti-rabbit Alexa 594-conjugated IgG (1:1,000) and goat anti-mouse Alexa 488-conjugated IgG (1:1,000) secondary antibodies for 1 h at room temperature.
6. Take images with a fluorescent microscope at 10x by automatic panoramic scanning at wavelengths of 594 nm and 488 nm, respectively (**Figure 6**).
    1. Turn on the fluorescence microscope, put the slide on the microscope stage, switch to the fluorescence channel, use the positioning key to position three to four points on the tissue, and focus to complete the shooting. After finishing shooting, save the images of different channels in the desired format, and then save the merged image.

Representative Results

To test the device's precision, the force that three different masses of weights made from the same height was measured using a peak pressure testing device. Twenty-four tests were carried out with varying groups of weights, resulting in (mean ± SD) 0.323 N ± 0.02 N for 1.3 g weights, 0.543 N ± 0.15 N for 2.0 g weights, and 0.723 N ± 0.26 N for 2.7g weights (**Figure 7**). Previous studies adopted dyne (dyn) or Kilodyne (Kdyn) as units to measure the contusion intensities. For better comparison with previous studies, the conversions between Newtons (N) and dyne/Kilodyne are listed (1 N = 1 kg × 1 m/s^2 = 1 × 10^3 g × 1 × 100 cm/s^2 = 1 × 10^5 dyn; 0.323 N = 32.3 Kdyn; 0.543 N = 54.3 Kdyn; 0.723 N = 72.3 Kdyn).

Table 1 and **Figure 4** show data of the lesions of the mild, moderate, and severe groups on coronal sections. Judging from **Figure 4**, on the 28th day post injury, the continuity of the distinguishable gray and white matter boundaries in the mild, moderate, and severe groups decreased successively, with the area of scar tissue growing larger and a mounting proportion on the cross-section of lesion center. There were obvious morphological differences in all the experimental groups compared with the normal group. This proved the rationality of the division of injury degrees in the experimental groups.

Table 2 and **Figure 5** describe injury of the spinal cord on the 1st and 56th days post-injury on sagittal sections. It can be seen that the area of lesion gradually increased significantly from the mild to severe groups on the 1st day post injury. Meanwhile, the continuity of white matter on both sides of the spinal cord was better in the mild group, with observable small round vacuoles, which are the characteristics of interstitial edema. In the moderate group, the white matter displayed poor continuity, and the structure of the ventral white matter was not ordered. In the severe group, the ventral white matter exhibited more severe disruption, and a large area of the cavity appeared in the center of the injury. Additionally, the surrounding tissue showed obvious filling of the red blood cells, and the red blood cells near the central canal gathered into strips. On 56th day after injury, scar formation was

observed in the injury center of the three groups, whose area increased according to the severity of the injury.

The integrity of spinal cord neurofilament on the 56th day post injury can also be derived from the analysis of the immunofluorescence staining results (**Figure 6**). The figure also shows that overlapping scar-forming astrocytes were visible in the center of all three groups of injuries, with the length of the injury area increasing with the severity of the injury, while the scar diameter decreased. This suggests the presence of scar contracture, which may lead to a decrease in spinal cord diameter.

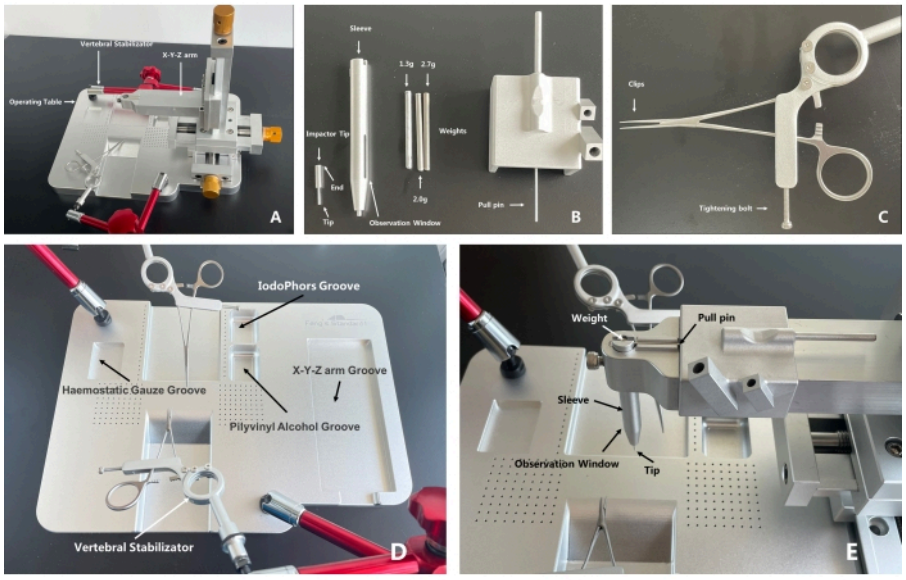

Figure 1: A whole and parts exhibition of the spinal cord injury coaxial platform. (**A**) The X-Y-Z arm and the operating table can be separated, which leaves adequate room for the operation procedure during which a small animal's spinal cord is exposed. The operating table can be moved freely during operation, reducing potential operating difficulty ascribed to position limitations. The body of the vertebral stabilizator has a three-joint universal arm for direction assistance, which increases its flexibility. (**B**) Put the impactor tip into the sleeve and assemble the latter into the X-Y-Z arm. Put the tip of the pull pin into the holes of the weight to prevent the weight from dropping and place the weight into the sleeve. With the parts assembled, locate the targeted injury area under the microscope. Then, lower the X-Y-Z arm until the end of the impactor tip is consistent with the lower level of the observation window, which indicates that a unified contusion height has been reached (the height between the weight and the impactor tip is 22 mm when the falling starts). Pull the pull pin, and the impact will be done. (**C**) After the injury area is exposed, use the clips to clamp and fix the spine of the mouse and the tightening bolt to stabilize the vertebral stabilizator. (**D**) Recommended functions for grooves on the operating table. The experimental animal is supposed to be put in the middle groove, with the head toward the anterior, thoracic part on the slope. The X-Y-Z arm is separated from the operating table. (**E**) A display of the assembled SCICP. Arrows indicate the parts. With the tip aiming at

the target contusion area, to start the contusion, pull out the pull pin, and the weight will drop onto the impactor tip to contuse the spinal cord. Please click here to view a larger version of this figure.

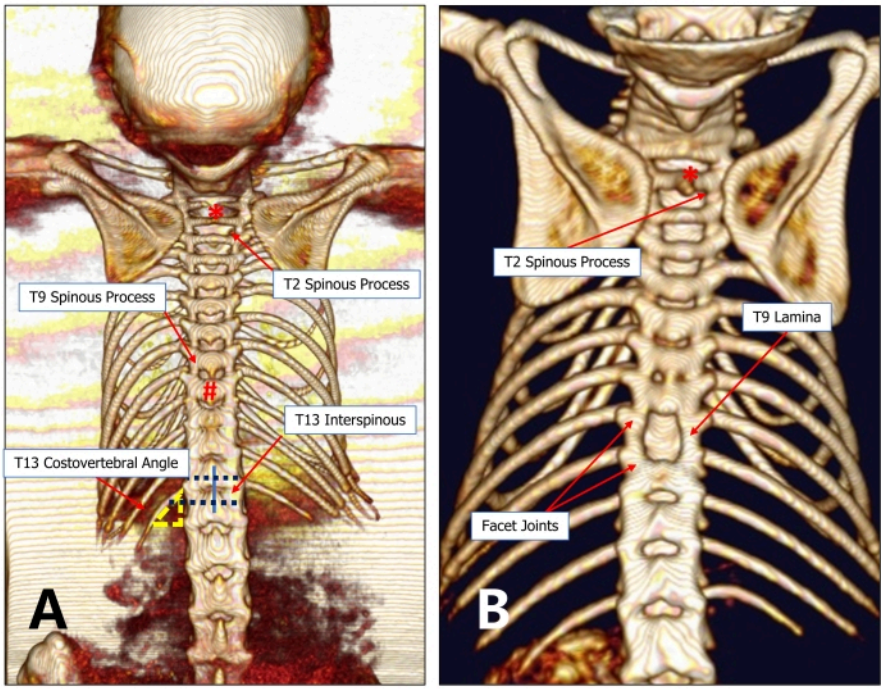

Figure 2: An imaging graph of the T13 costovertebral vertebra locating method. (**A**) The 13th rib and T13 are relatively constant anatomical structures. The T13 costovertebral angle can be easily detected under the microscope, from which the operator can probe toward the spinous process and find the T12-T13 interspinous space. Then, probe toward the rostral side successively to find the target injury vertebra (for example, T9). (**B**) A minimally invasive 9th thoracic laminectomy can preserve adequate lamina and facet joints between adjacent vertebral bodies. Please click here to view a larger version of this figure.

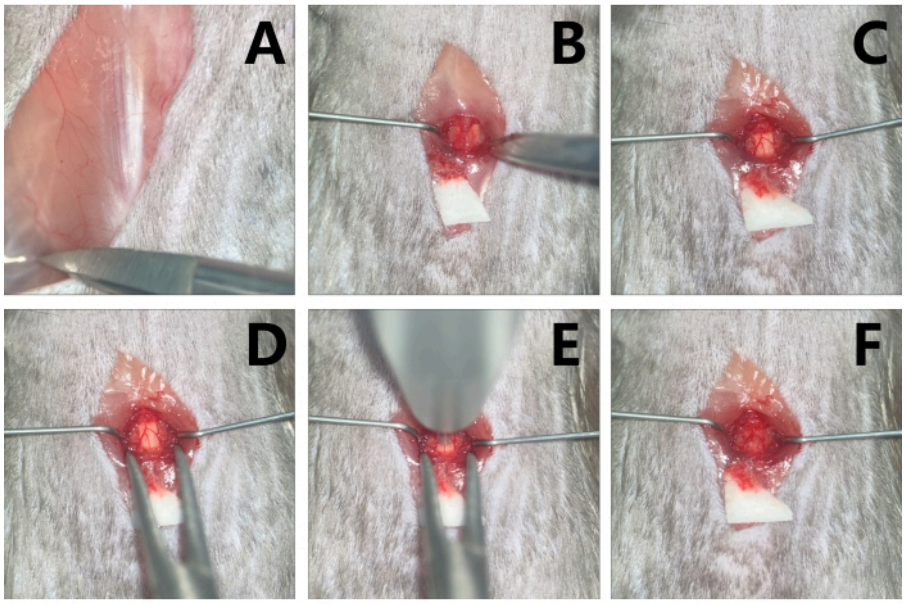

Figure 3: Exposure and contusion of the T9 level spinal cord in mice. (**A**) Probe the T13 costovertebral angle. (**B**) With the paraspinal muscle retracted by micro-retractors to make adequate space for operation, expose the T9. (**C**) Conduct T9 laminectomy with micro scissors. (**D**) Stabilize the vertebra with the clips of the vertebral stabilizator. (**E**) Aim at the target contusion area with the impactor tip. (**F**) Edema and congestion are noted in the injury area after contusion. Please click here to view a larger version of this figure.

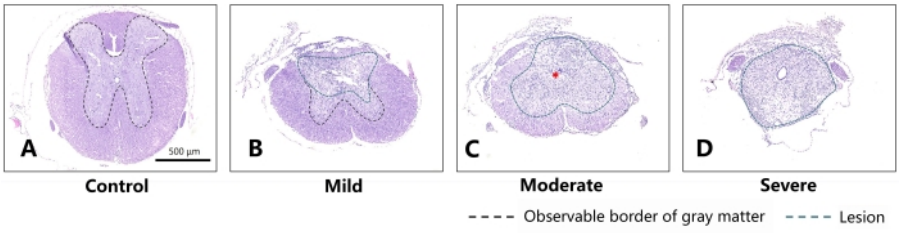

Figure 4: Representative sections on the 28th day after different degrees of SCI in mice (coronal sections). (**A**) Normal thoracic spinal cord of the mouse. Scale bar = 500 μm. (**B**) For the mild group, slight injury can be noted in the dorsal aspect of the spinal cord, while the morphology of the spared white matter and gray matter is substantially preserved. (**C**) For the moderate group, obvious scar tissue is observed in the spinal cord (indicated by the red asterisk). The differentiative characteristics between white matter and gray matter can barely be distinguished. (**D**) Comparatively, the spinal cord of the severe group has almost lost its original morphology and has almost been replaced by scar tissue. The green dashed line indicates the area of damage, and the black dashed line indicates the boundary of the observable gray matter. As the severity of injury increased, a larger lesion and less spared structure appeared in the mouse's spinal cord, with the border of gray matter barely distinguishable. Please click here to view a larger version of this figure.

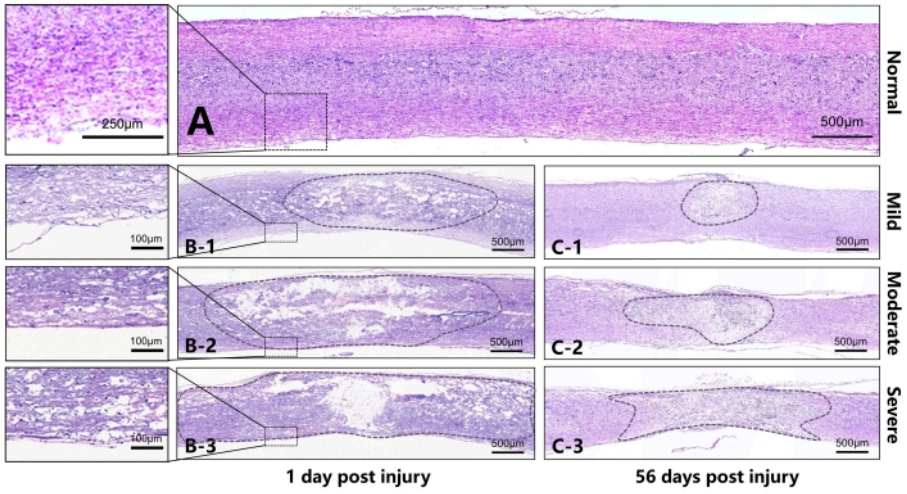

Figure 5: Representative sections on the 1st and 56th days after injury to the spinal cord of mice (sagittal sections). (**A**) Normal thoracic spinal cord of the mouse. (**B**) B1-B3 represent, respectively, the spinal cord on the 1st day after injury in the mild, moderate, and severe groups. It can be seen that, as the damage increased, a larger area was disrupted or liquified in the lesion center. The continuity of white matter in the ventral spinal cord differed due to different injury intensities. B1 shows that the white matter in the ventral spinal cord has better continuity with slight edema. B2 shows poorer continuity of the white matter in the ventral spinal cord and severer edema. The tissue in the center of the B3 SCI has lost almost all continuity, and there is extensive edema in the area outside the center of the injury. (**C**) C1-C3 represent, respectively, the spinal cord on the 56th day after the injury in the mild, moderate, and severe groups. Different degrees of scar contracture manifested in the injury center between different groups, and there was a significant difference in the diameter of the injury area. Scale bar = 500 μm. Please click here to view a larger version of this figure.

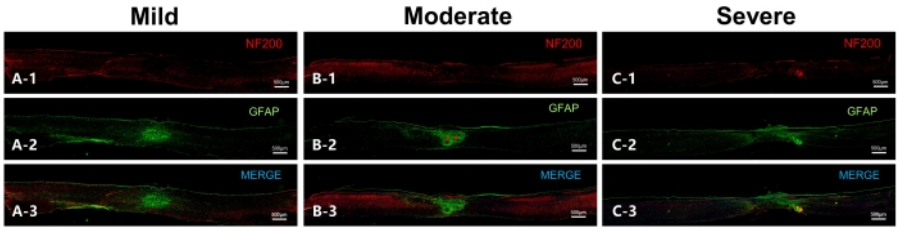

Figure 6: Representative sections on the 56th day after injury to the spinal cord in mice (sagittal sections). (**A**) Representative section of the mild group. NF200 indicates the neurofilament, while GFAP indicates astrocytes. Overlapping astrocytes are observed in the lesion epicenter, while the neurofilament in the ventral part of the spinal cord is in good continuity. (**B**) Representative section of the moderate group. Two scar centers can be observed (indicated by red asterisks) in addition to overlapping astrocytes, while the neurofilament in the ventral aspect has continuity. (**C**) Representative section of the severe group, with a large lesion range and massive scar-forming astrocytes. There is no obvious scar center observed, and the neurofilament has poor continuity. Scale bar= 500 μm. Please click here to view a larger version of this figure.

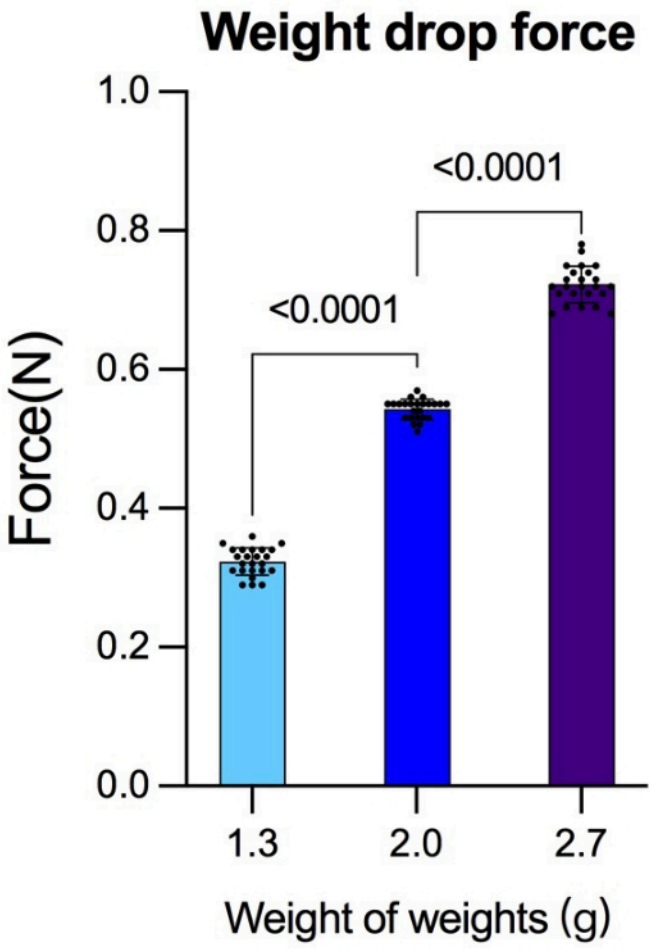

Figure 7: Force generated from the same height but with different weights. Before the experiment, the force generated by different masses of weights released from the same height was detected using a peak pressure detection device. After each group completed 24 detections, more reliable gravity data were obtained for the reference of striking force. The data were analyzed using the statistical software SPSS19.0. Data are presented as mean ± SD, n = 24 in each group. Comparisons among more groups were based on a one-way analysis of variance (ANOVA) used to test the differences; $p < 0.05$ was considered to be statistically significant. Please click here to view a larger version of this figure.

28 dpi			
Group	GMR (%)	WMR (%)	DR (%)
Normal	35.44	64.57	0
Mild	11.59	64.88	23.53
Moderate	0	41.14	58.86
Severe	0	0	100

Table 1: Rate of white matter, gray matter, and damage on the 28th day post injury. Abbreviations: dpi = days post-injury, DA = damaged area; GMR = gray matter rate; WMR = white matter rate; DR = damaged rate.

Group	1dpi DA (μm^2)	56dpi DA (μm^2)
Normal	0	0
Mild	2391250	666091
Moderate	4383381	1263191
Severe	5118833	1943962

Table 2: Comparisons between the lesion on sagittal sections on the 1st and 56th days post injury.

Discussion

Through the standardized procedure, stable data can be obtained, especially in small animal *in vivo* experiments, which can minimize the deviation of results caused by individual differences between the animals. Based on the above conditions and convenient application instruments, standardized, minimally invasive, accurate, and repeatable SCI models can be established.

Due to its practicability and convenience, previously, the weight drop impactor was used mostly[3]. The impactor introduced in this study shares the same principle with Allen's model[12]. Fortunately, due to the accurate manufacturing advantages of modern machining technology, the research team designed a weight drop impactor with the benefits of being easy to operate, strongly stable, and seldomly inaccurate. A peak pressure detection device was used to measure the gravity of different weights. Previous studies[6,10] about the Infinite Horizons impactor reported that a ±5 Kdyn range of force deviating from the intended force is accepted in the 30 Kdyn, 50 Kdyn, and 70 Kdyn groups, which provides a reference for the present study in terms of group division and contusion degree selection. In the present research, the possible force of different groups was measured in advance, and more accurate data were obtained.

More critical than the device in animal model experiments is the understanding and utilization of mouse anatomy. Making good use of anatomy can make procedures minimally invasive. Minimally invasive surgery directly affects

the stability of the functional state of the experimental animal and the consistency of subsequent mouse recovery. Previous studies have shown that the minimally invasive establishment of SCI models increases the stability of the vertebral structure and avoids additional damage caused by spinal instability during recovery in rats[1]. The premise of minimally invasive surgery is the reasonable use of natural anatomical structures. Therefore, the rapid and precise locating of spinal cord segments should be done in accordance with the anatomical structure of mice. As reported, the imaging method was used to find the vertebra[13]. Although it has high accuracy, in the actual experimental operation process, the imaging method for locating has the disadvantages of inconvenient operation, long operation time, complex equipment acquisition, and high equipment accuracy requirements. McDonough et al. described locating the T7 through the inferior angles of the scapulas[14], whereas mice act in a lie prostrate, so the inferior angles mentioned are supposed to be posterior angles. Moreover, using the lower scapular tips to find the T7 is a locating method for a specific position in human anatomy[15], which is not suitable for mice. Finally, Micro-CT data also validated the hypothesis that the posterior angles of the scapulae are not flush with T7 regardless of whether the mouse is in their natural or specific body position. McDonough et al.[14] also mentioned locating the highest point of the back when the mouse is arched and defining the highest point as T12. Comparatively, in the present research, the T9 is located with the assistance of T12-T13 interspinous space, which is neither associated with nor affected by the posture of the mouse. Besides, with this method, the target vertebra can be easily located and operated on. One should probe the 13th rib under the microscope, gently touch the area of the costovertebral angle, draw a line toward the spinous process, and then probe the space between the spinous processes of the T12-T13 toward the head. The research team used the T12-T13 interspinous space to locate the T9 of 12 mice. Finally, 12 female C57BL/6J mice had a Micro-CT scan after the T9 location and laminectomy. The result of the Micro-CT scan indicated that the removed laminae in all 12 mice were T9. The results of the Micro-CT showed that all the T9 were accurately located, and the accuracy was significantly higher than the scapula locating method. This method provides us with a fast and accurate way to locate, which contributes to the consistency of the injury model.

The minimal invasiveness of the present protocol is pronounced in mainly three aspects. Firstly, after locating, the paraspinal muscles at the T9 level are only retracted by micro-retractors, without damaging the muscles at the T8 or T10 levels. Besides, the exposure of the lamina by the micro-retractors does not interfere with the visual field. Second, blood loss, which is mostly from laminectomy, which may cause blood outflow from the cancellous bone, is very low in the operation procedure, almost no more than the volume to stain a 2 mm x 2 mm x 3 mm triangular piece of cotton. Thirdly, laminectomy was conducted limited to the needed area to the greatest extent, maintaining continuity of the lateral part of the lamina and greatly attenuating the vertebra instability. Compared to previous protocols[16,17], the present protocol reduces much unnecessary damage.

To evaluate the different degrees of SCI, the results between all groups in histopathology were compared with what previous studies have already shown[9,11,18]. These results are sufficient to complete an observational study of different degrees of injury and changes in different periods. HE and immunofluorescence showed that, with increases in the severity of SCI, more abnormal morphology appeared in the spinal cord tissue, and the increase in the degree of damage

also led to an increase in the degree of structural disorder of the spinal cord. From the perspective of tissue morphology observation, the degree and regularity of tissue morphology changes in each experimental group in this study are highly consistent with previous studies.

According to the current histological test results, clear changes in various indicators after different degrees of traumatic SCI are indicated, which further confirms the reliability of the model established in this study.

Accurate and effective though the technique is, potential limitations could exist for the methods. Regarding laminectomy, the operator should be skilled with operations under the microscope to prevent spinal cord being damaged by mistake. Also, the setup of the whole platform is based on mechanical structures, setting a higher demand for the operator compared to automized equipment. Indeed, all the mentioned problems can be improved by repeated training of the operation.

It can be seen that minimally invasive and standardized modeling is beneficial in making the results more uniform, stable, and repeatable, evaluating the efficacy of various treatment plans accurately, and optimizing the research plan for traumatic SCI.

Disclosures

Professor Shiqing Feng has ownership of the spinal cord injury coaxial platform.

Acknowledgments

This work was supported by the State Key Program of National Natural Science of China (81930070).

References

1. Duan, H. et al. A novel, minimally invasive technique to establish the animal model of spinal cord injury. *Annals of Translational Medicine.* **9** (10), 881 (2021).
2. Piao, M. S., Lee, J.-K., Jang, J.-W., Kim, S.-H., Kim, H.-S. A mouse model of photochemically induced spinal cord injury. *Journal of Korean Neurosurgical Society.* ***46*** .(5), 479-483 (2009).
3. Sharif-Alhoseini, M. et al. Animal models of spinal cord injury: A systematic review. *Spinal Cord.* **55** (8), 714-721 (2017).
4. Zhang, N., Fang, M., Chen, H., Gou, F., Ding, M. Evaluation of spinal cord injury animal models. *Neural Regeneration Research.* **9** (22), 2008-2012 (2014).
5. Borges, P. A. et al. Standardization of a spinal cord lesion model and neurologic evaluation using mice. *Clinics.* **73**, e293 (2018).
6. Ghasemlou, N., Kerr, B. J., David, S. Tissue displacement and impact force are important contributors to outcome after spinal cord contusion injury. *Experimental Neurology.* **196** (1), 9-17 (2005).
7. Siddall, P., Xu, C. L., Cousins, M. Allodynia following traumatic spinal cord injury in the rat. *Neuroreport.* **6** (9), 1241-1244 (1995).
8. Ford, J. C. et al. MRI characterization of diffusion coefficients in a rat spinal cord injury model. *Magnetic Resonance in Medicine.* **31** (5), 488-494 (1994).
9. Basso, D. M., Beattie, M. S., Bresnahan, J. C. Graded histological and locomotor outcomes after spinal cord contusion using the NYU weight-drop device versus transection. *Experimental Neurology.* **139** (2), 244-256 (1996).

10. Nishi, R. A. et al. Behavioral, histological, and ex vivo magnetic resonance imaging assessment of graded contusion spinal cord injury in mice. *Journal of Neurotrauma.* **24** (4), 674-689 (2007).

11. Ma, M., Basso, D. M., Walters, P., Stokes, B. T., Jakeman, L. B. Behavioral and histological outcomes following graded spinal cord contusion injury in the C57Bl/6 mouse. *Experimental Neurology.* **169** (2), 239-254 (2001).

12. Allen, A. R. Surgery of experimental lesion of spinal cord equivalent to crush injury of fracture dislocation of spinal column. *The Journal of the American Medical Association.* **LVII** (11), 878-880 (1911).

13. Kuhn, P. L., Wrathall, J. R. A mouse model of graded contusive spinal cord injury. *Journal of Neurotrauma.* **15** (2), 125-140 (1998).

14. McDonough, A., Monterrubio, A., Ariza, J., Martinez-Cerdeno, V. Calibrated forceps model of spinal cord compression injury. *Journal of Visualized Experiments.* (98), e52318 (2015).

15. Ernst, M. J., Rast, F. M., Bauer, C. M., Marcar, V. L., Kool, J. Determination of thoracic and lumbar spinal processes by their percentage position between C7 and the PSIS level. *BMC Research Notes.* **6**, 58 (2013).

16. Wu, X. et al. A tissue displacement-based contusive spinal cord injury model in mice. *Journal of Visualized Experiments.* (124), e54988 (2017).

17. Bhalala, O. G., Pan, L., North, H., McGuire, T., Kessler, J. A. Generation of mouse spinal cord injury. *Bio-protocol.* **3** (17), e886 (2013).

18. Shinozaki, M. et al. Novel concept of motor functional analysis for spinal cord injury in adult mice. *Journal of Biomedicine and Biotechnology.* **2011**, 157458 (2010).